

SANDIA REPORT

SAND2001-0999
Unlimited Release
Printed June 2001

Characterization of UOP IONSIV IE-911

May Nyman, Tina M. Nenoff, and Thomas J. Headley

Prepared by
Sandia National Laboratories
Albuquerque, New Mexico 87185 and Livermore, California 94550

Sandia is a multiprogram laboratory operated by Sandia Corporation,
a Lockheed Martin Company, for the United States Department of
Energy under Contract DE-AC04-94AL85000.

Approved for public release; further dissemination unlimited.



Sandia National Laboratories

Issued by Sandia National Laboratories, operated for the United States Department of Energy by Sandia Corporation.

NOTICE: This report was prepared as an account of work sponsored by an agency of the United States Government. Neither the United States Government, nor any agency thereof, nor any of their employees, nor any of their contractors, subcontractors, or their employees, make any warranty, express or implied, or assume any legal liability or responsibility for the accuracy, completeness, or usefulness of any information, apparatus, product, or process disclosed, or represent that its use would not infringe privately owned rights. Reference herein to any specific commercial product, process, or service by trade name, trademark, manufacturer, or otherwise, does not necessarily constitute or imply its endorsement, recommendation, or favoring by the United States Government, any agency thereof, or any of their contractors or subcontractors. The views and opinions expressed herein do not necessarily state or reflect those of the United States Government, any agency thereof, or any of their contractors.

Printed in the United States of America. This report has been reproduced directly from the best available copy.

Available to DOE and DOE contractors from
U.S. Department of Energy
Office of Scientific and Technical Information
P.O. Box 62
Oak Ridge, TN 37831

Telephone: (865)576-8401
Facsimile: (865)576-5728
E-Mail: reports@adonis.osti.gov
Online ordering: <http://www.doe.gov/bridge>

Available to the public from
U.S. Department of Commerce
National Technical Information Service
5285 Port Royal Rd
Springfield, VA 22161

Telephone: (800)553-6847
Facsimile: (703)605-6900
E-Mail: orders@ntis.fedworld.gov
Online order: <http://www.ntis.gov/ordering.htm>



SAND 2001-0999

Unlimited Release

Printed June 2001

Characterization of UOP IONSIV IE-911

May Nyman and Tina M. Nenoff

Environmental Monitoring and Characterization Department

Thomas J. Headley

Materials Characterization Department

Sandia National Laboratories

P O Box 5800

Albuquerque, NM 87185-0755

Abstract

As a participating national lab in the inter-institutional effort to resolve performance issues of the non-elutable ion exchange technology for Cs extraction, we have carried out a series of characterization studies of UOP IONSIV® IE-911 and its component parts. IE-911 is a bound form (zirconium hydroxide-binder) of crystalline silicotitanate (CST) ion exchanger. The crystalline silicotitanate removes Cs from solutions by selective ion exchange. The performance issues of primary concern are: 1) excessive Nb leaching and subsequent precipitation of column-plugging Nb-oxide material, and 2) precipitation of aluminosilicate on IE-911 pellet surfaces, which may be initiated by dissolution of Si from the IE-911, thus creating a supersaturated solution with respect to silica. In this work, we have identified and characterized Si- and Nb- oxide based impurity phases in IE-911, which are the most likely sources of leachable Si and Nb, respectively. Furthermore, we have determined the criteria and mechanism for removal from IE-911 of the Nb-based impurity phase that is responsible for the Nb-oxide column plugging incidents.

In parallel, UOP has revised the manufacturing process to eliminate or minimize these impurity materials, which are the sources of column plugging oxides. The primary

alteration in the manufacturing process is the addition of a NaOH wash of the IE-911 at the factory in a batch mode. A major thrust of the studies described here was to characterize these new materials (baseline—acid and leached—NaOH treated), specifically to determine if the leachable components had been minimized or removed.

Primary results include:

- The leachable Nb in the UOP-leached IE-911 was reduced by a factor of 20, compared to the original IE-911, acid-form materials (UOP batches 98-5, 99-7, 99-9).
- By TEM inspection, the soluble, Nb-based impurity phase is almost completely removed from the UOP-leached IE-911.
- There are single crystals of niobium oxide, several microns in diameter, abundant in both the baseline and leached IE-911 (which is regarded to be largely insoluble in NaOH, see first bullet). This impurity phase makes up less than a total of 1 % by volume of the IE-911.
- The leachable Si is determined to arise from trace impurities of silicate and aluminosilicate, incorporated into the IE-910 and IE-911 batches during the manufacturing process.
- These Si-containing impurities are not controllable, and vary in an unpredictable manner in composition, morphology, leachability and concentration between batches.

Finally, one additional sidelight study presented in this report is characterization of the binder, particularly its behavior in caustic solutions. The results of this study provided a better overall understanding of behavior and spectroscopic characterizations of IE-911.

CONTENTS

1.0 Introduction	6
2.0 Objectives	8
3.0 Characterization Studies	9
3.1 Instrumentation used for characterization studies	9
3.2 Leachable Elements in IE-911	10
3.2.1 Silicon-based Impurities.....	10
3.2.2 Niobium-based impurity: Ion Exchange and dissolution properties.....	11
3.3 Binder Characterization Studies.....	13
4.0 Characterization of UOP-Improved Baseline and Leached IE-911	19
4.1 Bulk Composition	19
4.2 Powder X-Ray Diffraction	20
4.3 Infrared Spectroscopy (binder characterization).....	21
4.4 Characterization of Morphology and Composition by Backscattering.....	21
Electron Imaging (BEI) and X-Ray Maps	
4.5 TEM Studies of baseline and leached IE-911 silicon and niobium impurities	23
5.0 Summary	26
6.0 Cited References	28
7.0 Acknowledgements	30

1.0 INTRODUCTION

The Department of Energy (DOE) is currently in the process of selecting a technology for ^{137}Cs removal from the Savannah River Site (SRS) salt wastes. The major competing technologies include non-elutable ion exchange, caustic side solvent extraction and small tank tetraphenylborate precipitation. The non-elutable ion exchange technology utilizes an inorganic sorbent, UOP IONSIV[®] IE-911 (manufactured by UOP LLC, Des Plaines, Illinois), in a column operation. The IE-911 sorbent is composed of zirconium-hydroxide-bound crystalline silicotitanate (CST). The CST ion exchanger is an inorganic material with superior properties for this application including: 1) excellent Cs selectivity in the presence of high concentrations of competing ions (i.e. Na), 2) stability in extreme chemical environments (acidic or caustic solutions) and 3) stability in extreme radiation fields.¹

Recent column testing of the IE-911 carried out at ORNL and SRS have given test results that have raised some issues concerning the performance of these materials in particular chemical environments. The incidents relevant to this current report are all column pluggings. They are summarized in an interoffice memorandum by D. D. Walker in August 2000² and described below. In one incident, IE-911 pretreated with NaOH formed Nb-rich solids that plugged the top layer of a column.³ Analyses of the pre-wash solutions also show high concentrations of Nb. Second, it was observed that IE-911 exposed to alumina-containing simulant (i.e. average salt simulant) nucleated the growth of sodium aluminosilicate phases such as cancrinite on the surface of the bound pellets. This resulted in partial cementation and interstitial space filling (as well as some drop in Cs K_d).⁴

As part of an inter-institutional effort to understand and resolve these performance issues, our team at Sandia National Laboratories has been carrying out characterization studies of IE-911 (acid form, base treated and simulant exposed). The first portion of this work (summarized in the previous interim report⁵) involved characterization of UOP batches 98-5, 99-7 and 99-9, which were the materials in service at the time of the column plugging incidents. Highlighted results of the previous report include: 1) aluminosilicate precipitation was identified as the cause for Cs K_d drop, 2) the time/temperature boundaries for CST thermal stability in simulant were identified, and 3) Nb- and Si-based impurities were identified which may be related to the niobium-oxide and aluminosilicate plugging incidents, respectively. The impurities are likely at the root of the column-plugging incidents because they are easily leachable sources of Nb and Si, respectively, and therefore quickly supersaturate the NaOH or simulant solutions with these oxides. In the case of Si, the average simulant is already almost saturated with respect to Si ($\sim 0.004\text{ M}$)⁶. Therefore, the dissolution of more Si from the IE-911 likely pushes the solutions to supersaturation and, consequently, results in aluminosilicate precipitation.

In response to the plugging issues and the positive identification of impurity phases as probable causes of the plugging incidents, UOP has since re-engineered the IE-911 in an attempt to eliminate the sources of these problems. Manufacturing alterations which were discussed by UOP and SRS personnel include: a post IE-910 synthesis caustic wash,

altered binding chemistries (acid strengths, etc.), and post-binding IE-911 caustic wash. According to UOP personnel, the post-binding IE-911 caustic wash was the only manufacturing alteration implemented. However, routine characterization of these re-engineered materials revealed some inconsistencies with previous batches, perhaps due to factors that are not controllable by UOP (i.e. state of precursors for IE-910/911 synthesis). Major differences observed between previous UOP batches (98-5, 99-7, 99-9) and the re-engineered materials include: 1) Different Nb-containing impurities than observed in previous IE-911 batches (see section 4.4.5) and 2) Slightly different binder characteristics. These re-engineered materials are referred to collectively as the pre-production batch (including the IE-910). Pre- and post- caustic washed IE-911 materials are called 'baseline' and 'leached', respectively.

2.0 OBJECTIVES

In the CST Process Research Roadmap, this work falls under item 7.2.3.5, Revised Manufacturing Process (CST SOWM 2.1) since it describes the test on the new material that verifies if the new manufactured material resolves the leaching problems.⁷

The objectives of this body of work are:

- 1) To understand and resolve the performance issues, particularly column plugging issues.
- 2) To characterize the binder material in order to round out our knowledge on IE-911 properties, behavior, and spectroscopic 'fingerprints'.
- 3) To determine if UOP's implemented manufacturing alterations have successfully removed leachable impurities, which ultimately result in column plugging.

These issues were addressed by the following actions:

- 1) Silicon-based impurities in IE-911 (which may be related to aluminosilicate precipitation) were identified and characterized.
- 2) The niobium-based impurity phase as a source of excessive Nb leaching was identified and characterized, particularly with regard to its ion exchange/solubility properties.
- 3) Development of a protocol for removal of niobium-based impurity phase from IE-911 was investigated.
- 4) Binder material was synthesized and characterized, and its stability in caustic solutions was investigated.
- 5) Finally, systematic characterizations of the new baseline and leached IE-911 were carried out to determine if the manufacturing alterations produced the desired changes in material properties (i.e. reduced Nb leaching and elimination of the impurity source of excessive Nb leaching).

3.0 CHARACTERIZATION STUDIES

3.1 Instrumentation used for characterization studies

Samples for X-ray Powder Diffraction (XRPD) were ground using a mortar and pestle and mounted as a loose powder in a well-type Probering sample holder. The diffraction data were obtained from a Bruker AXS D8 Advance instrument with a Cu-K α source and solid-state (Kevex) detector. Data were collected in the range of $2\theta = 5\text{-}60^\circ$ with a step size of 0.05° and a step time of 5 seconds. Samples were rotated (~ 30 rpm) during data collection to eliminate the effects of specimen inhomogeneities.

Direct Coupled Plasma Spectroscopy (DCP) Analyses were obtained from a FISIONS instrument SS-7 DCP equipped with a plasma argon-air flame. Powder samples of IE-911 for wet chemical analysis were digested in 40% HF and diluted with DI water. For the elements Si, Ti, Nb and Zr, 5 and 20-ppm aqueous standards were prepared by appropriate dilutions of the 1000-ppm SPEX Plasma standards. Similarly, 2 and 6-ppm standards were prepared for Na. To eliminate matrix effects for the Nb analyses, it was necessary to add Na, Si, Ti, and Zr to the Nb standards in relative concentrations equivalent to those that are found in the IE-911 samples. To account for drift correction, standards were run before and after analyses and sample concentrations were corrected using a time-concentration curve.

Differential Thermal Analysis-Thermogravimetric Analysis (DTA-TGA) experiments were performed on an STD 2960 TA DTA-TGA instrument with alumina as a standard for DTA. Samples (10 - 15 mg) were heated at $10^\circ\text{C}/\text{min}$ to 900°C . Argon was used as a sweep gas with a flow of 20 cc/min.

Transmission Electron Microscopy/Energy Dispersive Spectroscopy (TEM/EDS) Samples are prepared for TEM analysis by grinding a small quantity of the pellets in butanol and dispersing the slurry to dry on lacey carbon substrates on Cu support grids. TEM imaging, electron diffraction, and elemental analysis of phases in the samples are performed at 300 kV on a Philips CM30 TEM equipped with an Oxford Instruments EDS spectrometer with a low-Z window to facilitate light element analysis.

Infrared (IR) Spectroscopy. Samples for IR Spectroscopy were ground with CsI (1-3 wt % IE-911 in CsI matrix) and pressed into a pellet. Data were collected on a Perkin-Elmer Spectrum GX FTIR System in the mid-IR range ($370\text{-}7800\text{ cm}^{-1}$), 20 scans.

3.2 Leachable Elements in IE-911

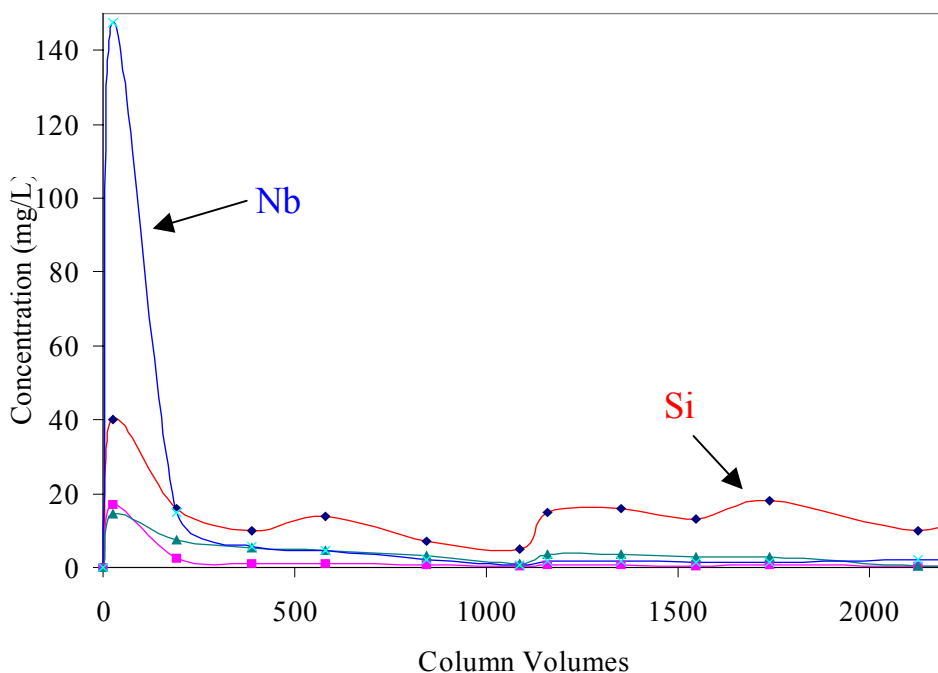


Figure 1. Leached components from IE-911, UOP batch 99-9 during NaOH-column washing.⁷

It was noted in the earlier batches of IE-911 (i.e. UOP batches 98-5, 99-7 and 99-9) that some elemental components, particularly Nb and Si, exhibit unusually high leach rates or leach patterns that do not reflect the leach behavior of the known components of IE-911 (CST plus binder). **Figure 1** shows the IE-911 elements, Nb, Si, Ti, and Zr, leached from IE-911, batch 99-9, during column washing pre-treatment.⁸ Labeled are the leach curves (concentration vs. column volumes) for Nb and Si. There is an initial spike of leached Nb that reaches a maximum of about 150-ppm, compared to around 20 ppm for Zr and Ti. The Si has a much lower initial spike of approximately 40-ppm, but then leaching is sustained with continued column washings (at around 10-20 ppm). In comparison, the concentration of leached component of the other elements drops off to very minimal with subsequent column washings. The behavior of the Nb is consistent with a base-soluble niobium-containing impurity, which was found to be the case (see section 4.2.2). The behavior of Si is consistent also with a Si impurity, which perhaps alters to a less soluble form when exposed to NaOH. This is the conclusion that is drawn from the observations made below (section 4.2.1).

3.2.1 Silicon-based Impurities

By transmission electron microscopy (TEM), we observe in the as-received (acid form) IE-911 (UOP batch 99-7), ~50 nm diameter amorphous silica impurities and are often aggregated with amorphous alumina. For instance, **figure 2a** shows an aggregate

(indicated by the arrow) which is 80% silica and 20% alumina, as determined by EDS. In

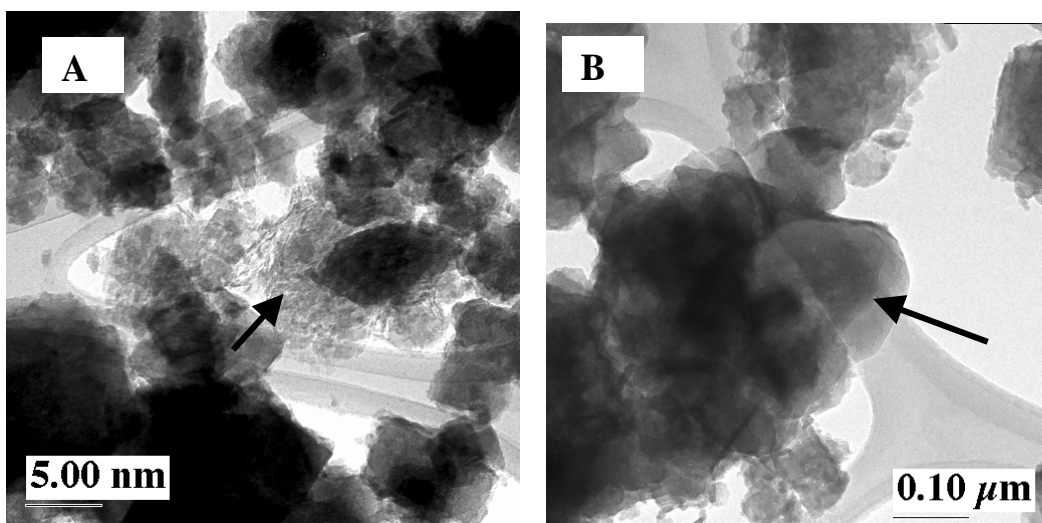


Figure 2. TEM images of: **a.** Amorphous silica–alumina aggregate impurity in acid form of IE-911 (UOP batch 98-7). **b.** Crystalline aluminosilicate impurity in NaOH-treated IE-911 (UOP batch 98-7), apparently formed by the reaction of the silica–alumina aggregate with NaOH.

the NaOH-treated IE-911 (**figure 2b**, indicated by the arrow), the silica-alumina aggregate is reacted to form a crystalline aluminosilicate phase. This observation is consistent with the continued silica leaching with subsequent column washings, whereas the leachability of the other IE-911 components drops off. Since the silica is changing form and reacting, its solubility properties are evolving as well.

3.2.2 Niobium-based impurity: Ion exchange and dissolution properties.

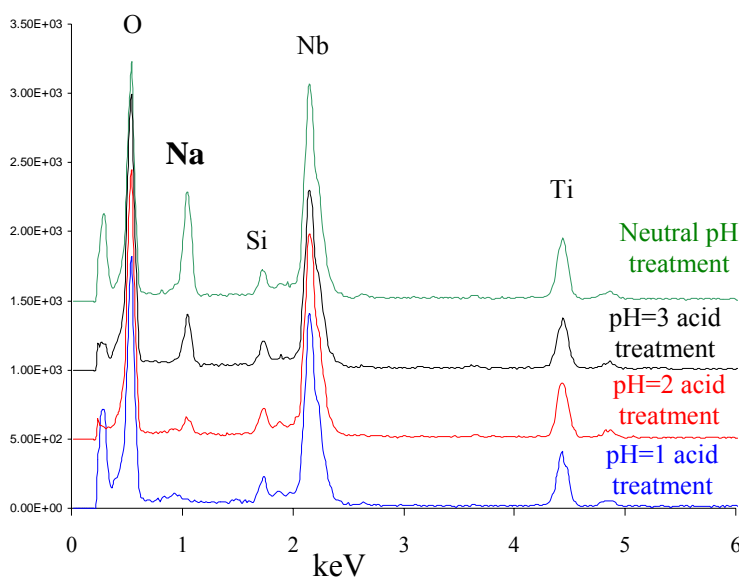


Figure 3. Energy dispersive spectra (EDS) of IPX showing decreasing Na content with increasing acidity of acid treatment while the concentration of the other elements remains constant. This is consistent with an ion-exchange process as a mechanism of Na removal. The top EDS spectrum (IPX with neutral pH treatment) is the equivalent of IPX before any treatment is implemented.

In the course of TEM characterization studies of IE-911, we have noted a crystalline impurity phase that contains Na, Ti, Si, Nb and O, with Nb being the predominant metal. This phase has been frequently noted as a byproduct of CST hydrothermal synthesis by both bench-scale synthesis⁹ and industrial-scale synthesis¹⁰. If this impurity is present in high enough

concentration ($\sim >5\%$), it is identified by peaks ($2\theta = 8.5^\circ$ and 10.0°) in the X-ray diffraction pattern of as-synthesized CST. This portion of the report describes experiments carried out to document the fate of this phase upon exposure to acid followed by exposure to base. It is this sequence of chemical exposure that this impurity phase experiences during the CST acidic binding process followed by the NaOH column-treatment, where the NaOH column-treatment step can result in formation of a niobium-oxide, column-plugging precipitate.

For this study, we used IE-910, the unbound CST, for the source of the Nb-based impurity phase. The phase is called 'IPX', or impurity phase X, for the sake of this discussion. First, IE-910 was exposed to an acid wash in four separate experiments (pH = 1, 2, 3 and neutral). The acid washes were carried out with IE-910 in contact with aqueous nitric acid solutions of the appropriate pH, which were shaken at 300 RPM for four hours at room temperature. Following the acid wash step, the IPX contained in the acid washed IE-910 was examined by TEM/EDS to document changes in composition and morphology. Next, the previously acid-treated IE-910 was exposed to 1 molar NaOH solution overnight at room temperature and examined by TEM/EDS again. The EDS spectra of IPX contained in post-acid treated IE-910 are shown in **figure 3**. There is a corresponding decrease in Na content with increasing acidity of the acid wash. The

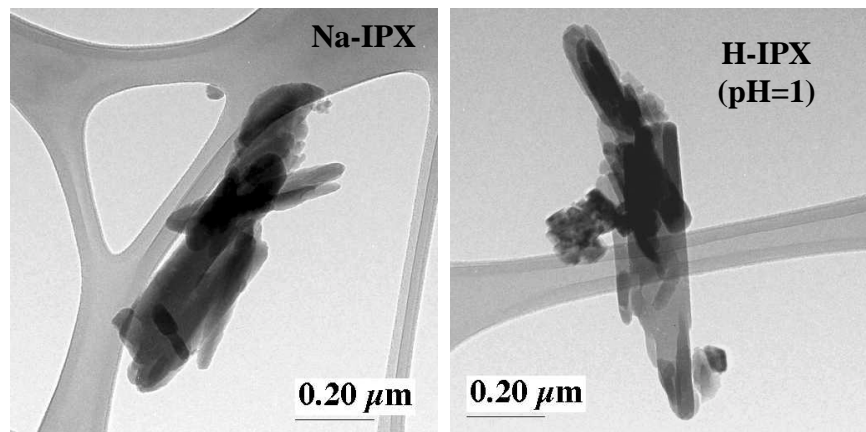


Figure 4. TEM images of IPX, untreated (left) and following acid-wash of pH=1 (right), showing no morphology change accompanies acid treatment and corresponding decrease in sodium content (see figure 3).

relative concentrations of the other elements remain constant. Furthermore, the morphology of the acid-treated IPX remains unaltered with the change in Na concentration (**figure 4**). These two observations are consistent with an ion-exchange mechanism (exchange Na^+ for H^+) for removal of Na from IPX in the acid wash step. Observations by TEM of the four acid-washed IE-910 samples subsequently exposed to 1 molar NaOH solution include the following: The IPX phase in the previously pH=1 acid-treated sample was completely removed (dissolved). For each of the other experiments (of higher pH acid treatment), the IPX was still present following base wash, and the IPX composition matched that of the IPX before acid-treatment (i.e. the Na concentration was increased). Examination of IPX compositions following acid-wash (**figure 3**) reveals the

pH=1 acid treatment was the only experiment in which Na was completely removed. In the case of the acid treatments of pH = 2 and 3, a base treatment following the acid treatment resulted in re-sorption of Na into IPX (i.e. reversible ion exchange). However, in the case of an acid treatment of pH=1, a base treatment following the acid treatment resulted in dissolution of IPX, rather than re-sorption of the Na (irreversible ion exchange). Therefore, this suggests that complete removal of Na from IPX alters the framework structure so that Na cannot be re-sorbed. Furthermore, the pH=1 acid treatment produces a material which is soluble in caustic solution.

These studies show that it is this acid treatment (binding process) of IPX followed by base treatment (column conditioning) that solubilizes the IPX and results in reprecipitation of a column plug. The report by Krumhansl et al.¹¹ reveals that the solubility of the column-plugging oxide (hexaniobate) decreases with increasing pH, which is also consistent with formation of a column plug. As the NaOH wash solution neutralizes the acidic IE-911, the pH of the solution first drops and then slowly increases, which subsequently results in precipitation of the column plugging Nb-oxide. A corollary examination of as-received (acid form of UOP batch 99-7) and NaOH-treated (UOP batch 99-7) IE-911 revealed that the IPX in the as-received IE-911 contains no sodium and that IPX is absent from NaOH-treated IE-911. Based on these studies, the recommendation for avoidance of Nb-oxide column plugging is 1) treat the CST with a high acidity wash (pH=1), followed by an NaOH treatment in the batch mode. This latter step has been addressed by UOP in their revised manufacturing process.

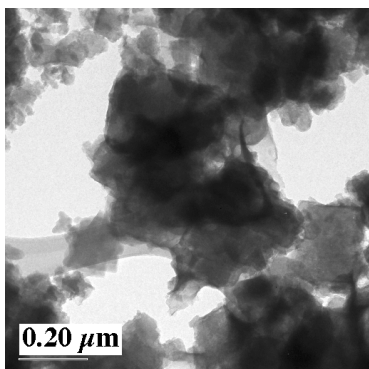


Figure 5. TEM image of overgrowth morphology observed in approximately 25 vol. % of NaOH-treated IE-911 and not observed in the as-received, acid form of IE-911.

3.3 Binder Characterization Studies

During the course of initial IE-911 characterization studies, 'overgrowth' morphology was noted by TEM investigations of the binder of NaOH-treated IE-911. This morphology was not observed in the acid form of IE-911. This morphology, which was observed in approximately 25% of the binder material, is documented in **figure 5**. The observation of this phenomenon led to the binder studies described in this section. In addition to investigating the cause of this 'overgrowth' morphology, we were interested in defining the spectroscopic fingerprints of the binder in IE-911, as well as

determining its behavior in highly caustic solutions. By investigating the binder alone (without CST), we are able to provide a more complete understanding of IE-911 spectral characterizations in which the contributions from the binder are difficult to distinguish from those of the CST (i.e. infrared spectroscopy, thermogravimetry).

Binder material synthesis was carried out using the same chemical precursors and general procedure used by UOP.¹⁰ A zirconium nitrate was added to 1000 ml water and stirred and heated. Nitric acid was added to adjust the pH to 1.64. The mixture (50 °C) was stirred overnight and filtered to remove any undissolved solids. Ammonium hydroxide

solution (40 wt %) was added to obtain a white flocculent precipitate of zirconium hydroxide. The product was separated from the solution by filtration, rinsed with hot water and air-dried. The zirconium hydroxide (2.8 grams) was collected and characterized by X-ray diffraction, infrared spectroscopy, thermogravimetric analysis (TGA) (water/hydroxyl content) and DCP spectroscopy (Zr content). These characterizations confirmed the material to be amorphous $Zr(OH)_4$.

The $Zr(OH)_4$ was then exposed to 3M NaOH solution for up to 5 days at 50 °C. In these experiments, we were looking specifically for evidence of dehydration of the $Zr(OH)_4$ via oxo cross-linking or ion exchange reactions, as shown in equations 1 and 2.



Both reactions would result in a decrease in volume of the binder and possibly contribute to the overgrowth morphology observed in the NaOH-treated binder observed in **figure 5**. A secondary reason for this study was to investigate the cause of the cracking/shelling of the NaOH-treated pellets when exposed to heat and vacuum, a phenomenon not observed in pellets which had not been previously exposed to caustic solutions or simulant solution.⁵ If the binder dehydration-condensation reactions do occur as a result of NaOH treatment, then this phenomenon may result in shrinkage of the binder and formation of a more friable and brittle material.

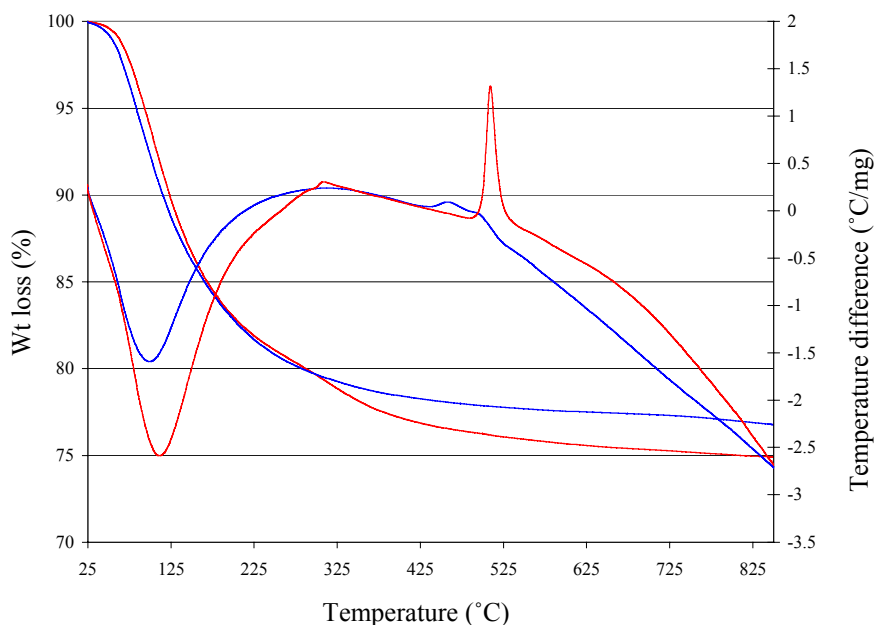


Figure 6. TGA-DTA curves of untreated binder (red) and binder that has been treated with NaOH for 5 days at 50 °C (blue).

Powder X-ray diffraction of the binder and NaOH-treated binder revealed amorphous material, as expected. Wet chemical analysis (DCP) of the Na and Zr contents of the NaOH-treated binder material showed essentially no Na is incorporated into the zirconium-hydroxide matrix by ion exchange or any other mechanism. Thermogravimetric-differential thermal analysis (TGA-DTA) of the binder and NaOH-treated binder are shown in **figure 6**. The as-

precipitated binder has a weight loss of 25% and a sharp exothermic phase transition around 520° C, which correspond with crystallization of tetragonal ZrO₂ (determined by X-ray diffraction of the heat-treated material). The 25% weight loss is consistent with a chemical composition of Zr(OH)₄ (calculated weight loss = 23% to convert Zr(OH)₄ to ZrO₂). The NaOH-treated Zr hydroxide undergoes an approximate 23% weight loss. The phase transition takes place approximately 50° C lower than the former and it is not as exothermic. The combined TGA-DTA and DCP analyses of the binder material and NaOH-treated binder material suggested that exposure of binder material to NaOH solution does not result in dehydration reactions such as oxo-cross-linking or ion-exchange. However, IR spectroscopy investigations and revisiting the TGA-DTA data to help understand the IR data revealed that changes in the binder do indeed occur as a result of NaOH treatment which are described below.

Figure 7 shows IR spectra of (from top to bottom): 1) IE-910, Na-form, 2) IE-911 acid form (99-7; as received) 3) IE-911 Na form (99-7, NaOH treated) 4) Zr(OH)₄, NaOH-treated, and 5) Zr(OH)₄, as precipitated. In the IE-910 spectrum (just CST, no binder) there is a sharp band at 1630 cm⁻¹. This is the H-O-H bending frequency of the pore water of CST. In the spectrum of the Zr(OH)₄ (bottom), there is a broad adsorption from ~1200 cm⁻¹ and below which is characteristic of the Zr-O lattice vibrations, and the higher frequency shoulder around 1000-1200 cm⁻¹ which is the bending mode of Zr-OH bonds.¹²⁻¹⁴ These broad bands are observed in IE-911 (binder plus CST), acid and NaOH-treated forms. In IE-910, the bands of the Si-Ti-Nb-O CST framework below 1200 cm⁻¹ are relatively sharp, since CST is a crystalline (ordered) material.

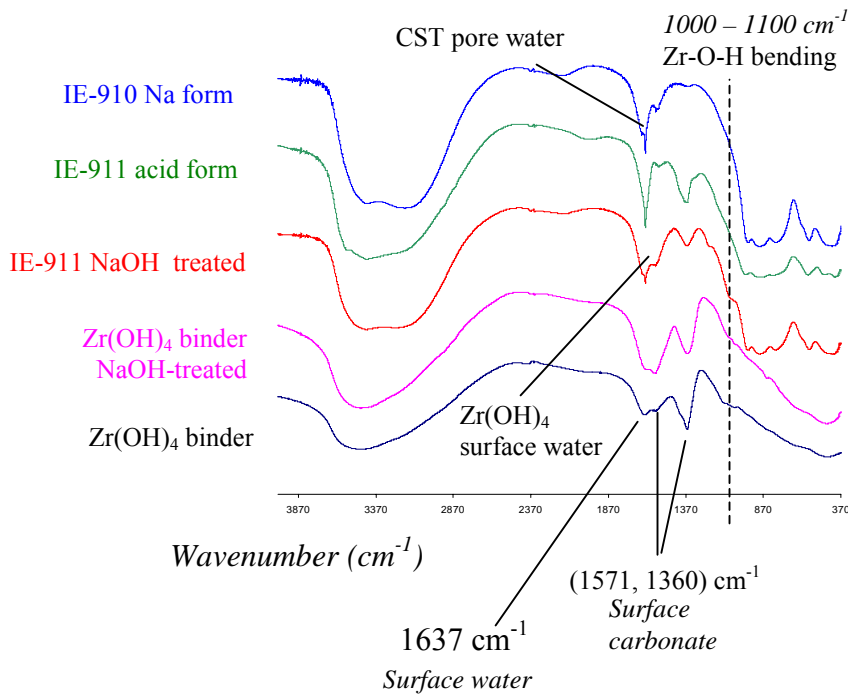


Figure 7. IR spectra of various forms of IE-910, IE-911 and Zr(OH)₄ binder material revealing the variation in binder features with exposure to NaOH solutions.

Comparably, this region is broadened in the direction of higher frequency in the IE-911, due to the overlap with the bands of amorphous binder. In the $Zr(OH)_4$ (both as-precipitated and NaOH-treated) and the IE-911, there are also bands around 1570 and 1360 cm^{-1} which are characteristic of surface-adsorbed carbonate. Zirconium oxide (and presumably zirconium hydroxide) has a great affinity for adsorbing carbon dioxide in ambient atmosphere.¹³ Also, there is a broad H-O-H surface water bending vibration observed in the spectra of $Zr(OH)_4$ and bound CST (IE-911). In both the NaOH-treated $Zr(OH)_4$ and the NaOH-treated IE-911, the carbonate bands become diminished compared to the carbonate bands of the acid form of IE-911 and the as-precipitated $Zr(OH)_4$. This is easily understood, in that the carbonate dissolves as predominantly CO_3^{2-} upon base treatment. In fact, an alkaline wash is a known method of removing carbonate from metal oxide catalyst surfaces.¹³

The H-O-H bending frequency at 1630 cm^{-1} of the surface water increases in intensity with NaOH treatment of both the $Zr(OH)_4$ and the IE-911. This suggests NaOH treatment result in sorption of more surface water. Additionally, the Zr-OH bending region (shoulder around $1000\text{-}1200\text{ cm}^{-1}$) changes slightly with NaOH treatment. This change is more pronounced in the new baseline and leached, pre-production batches (see below, section 4.4.3). Changes in these two IR regions in response to NaOH-treatment suggest changes in surface morphology of the $Zr(OH)_4$ affects the availability of surface sites for water sorption. A mechanism for NaOH-alteration of the $Zr(OH)_4$ surface accompanied by increased water sorption is illustrated in **figure 8** below:

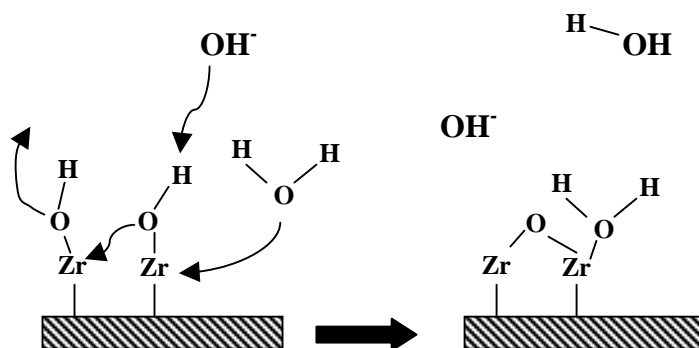


Figure 8. Schematic illustrating a possible mechanism for sorption of water on a $Zr(OH)_4$ surface when treated with NaOH, which would also retain the same overall water content of the material (see text and TGA results).

This schematic shows dehydration by oxo-formation, also described in equation 1. In this proposed mechanism, upon exposure to NaOH solution, an H^+ is removed from the surface by a hydroxyl in solution. The O^{2-} then bridges to a second Zr (oxo bridge formation), accompanied by elimination of an OH^- from the second Zr. This elimination reaction results in more accessible Zr sites for surface sorption of molecules such as water. This type of elimination reaction is called base-catalyzed condensation, and is a common reaction in sol-gel formation of oxide/hydroxide materials from metal

alkoxides¹⁵. Both the TGA data and IR data are consistent with this model. The TGA of $Zr(OH)_4$, before and after NaOH-treatment (**figure 6**), shows minor change in bulk water content. This elimination reaction accompanied by sorption of surface water (indicated by the IR) has no net change in bulk water content. The IR spectra also show some change in the Zr-OH bending mode in both the NaOH-treated $Zr(OH)_4$ and NaOH-treated IE-911, although an exact interpretation of this region of the spectra is not easily accomplished due to the overlap of many broad bands in this region of the spectrum. The DTA results (**figure 6**) are also consistent with this explanation of the IR results. Since NaOH-treatment results in partial condensation by oxo formation, there is a smaller kinetic barrier to formation of the zirconium oxide phase. Therefore the zirconium oxide phase can form at a lower temperature by a less endothermic process. Another NaOH- $Zr(OH)_4$ reaction was first described by Clearfield, which is worth noting in this discussion.¹⁶ The $Zr(OH)_4$ is slightly soluble in base as $Zr(OH)_5^-$. This local dissolution and reprecipitation process results in increased ordering of the zirconium hydroxide tetrameric building blocks into sheets and thus increased formation of O-H bridges.

One may alternatively argue that the changes in surface water and the Zr-O-H bending modes may be a result of removal of the sorbed carbonate ions. However, this is less likely since the hydroxyl anions are expected to be much more abundant than the carbonate anions, since the hydroxyls are stoichiometric part of the bulk material and the carbonates are only surface anions.

The more ordered, cross-linked and partially condensed NaOH-treated $Zr(OH)_4$ material may exhibit increased or decreased binder strength. The strength may increase by cross-linking or decrease by becoming more brittle. The increased brittleness may be responsible for the observed cracking of NaOH-treated IE-911 upon exposure to heat and vacuum.

Finally, the synthesis of binder material using the general procedure described by UOP produced a material consistent with a $Zr(OH)_4$ formula, which suggests this is the formula of the IE-911 binder. Prior to this study, the binder has been described, at best, generally as an oxy-hydroxide with an approximate formula $ZrO_x(OH)_{4-x}$ ($x = 0-3$).

In summary, these studies reveal:

- The binder material has a chemical formula of $Zr(OH)_4$
- Spectroscopic evidence suggests that upon exposure to NaOH solution, the binder material may undergo base-catalyzed condensation reactions by oxo-cross-linking.
- Surface water increases on the binder material upon exposure to NaOH solution
- The binder material may also undergo hydroxyl cross-linking, likely by local dissolution-reprecipitation reactions
- These NaOH-binder reactions may involve slight volume reduction and therefore be responsible for both the ‘overgrowth’ morphology observed by TEM and the cracking/shelling of the NaOH-treated pellets upon exposure to NaOH or simulant solution

- This hydroxyl cross-linking may therefore affect binder behavior in certain environments (i.e. dry heating)

4.0 Characterization of UOP-improved Baseline and Leached IE-911.

The remainder of this report is a summary of characterization studies of the UOP-improved IE-911, baseline and leached. In addition to routine characterizations such as X-ray diffraction and elemental analyses, these studies are particularly focused on examination of impurity phases. The main focus of this portion of the study is to determine if the altered manufacturing processes has minimized or eliminated these impurities.

4.1 Bulk Composition

The baseline and leached IE-911 samples were analyzed for Na, Ti, Si, Zr, and Nb by DCP spectroscopy. The results are summarized below in **Table 1**.

Table 1. Calculated and Observed Composition of Baseline and Leached IE-911.

Sample	Formula wt	Wt% Ti	Wt% Ti	Wt% Si	Wt%Si	Wt%Zr	Wt% Zr	Wt%Na	Wt%Na	Wt%Nb	Wt%Nb
		(calc)	(DCP)	(calc)	(DCP)	(calc)	(DCP)	(calc)	(DCP)	(calc)	(DCP)
Baseline	771.9	17.41	17.78	7.26	7.65	10.96	11.24	2.98	2.57	15.03	15.36
Leached	815.9	16.47	16.27	6.86	7.46	10.37	10.21	8.46	10.03	14.22	13.17

The ‘DCP’ wt % is what was observed experimentally. The ‘calc’ wt% is calculated based on the formula:

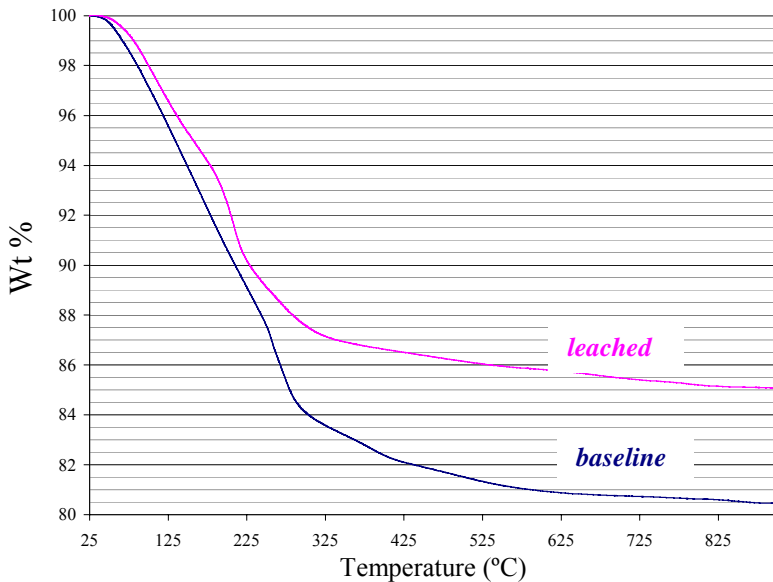
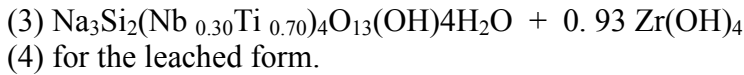
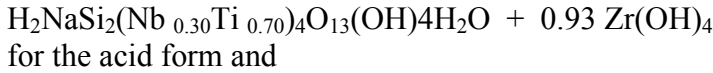


Figure 9. Thermogravimetric curve of baseline and leached IE-911.

The Ti:Nb ratio was determined by DCP. The remainder of the CST formula is defined by the CST structure. The ratio of CST to binder unit was determined by the ratio of Ti:Zr (3.00) in both the acid and NaOH-treated forms. The calculated and observed (DCP) concentrations of each component agree within 1%. Therefore, by these analyses, the impurity

phases observed by SEM and TEM do not constitute a significant portion of the bulk material. The niobate-based impurity phases in the acid form are likely to be fairly minor since the observed (DCP) Nb concentrations are as expected. The Ti:Nb ratio is also the ratio expected, based on the work of Dosch and Anthony¹⁷ on determining the maximum substitution of Nb into the Ti site in the CST framework.

The thermogravimetric curves for the baseline and leached IE-911 are shown in **figure 9**. The observed and calculated weight losses (in wt%) are 1) leached: obs. = 15.0, calc. = 14.0 and 2) baseline: obs. = 18.5, calc. = 17.2. The volatile component of both materials is water, which originates from the hydroxyls in the binder and the pore water and framework hydroxyls of the CST. The baseline form contains (and thus releases upon heating) more volatile components than the leached form, due to the volatile protons in the baseline form compared to the non-volatile sodium cations in the leached form. Finally, the observed water content was slightly greater than the calculated water content for both materials. This is likely due to the presence of surface water.

4.2 Powder X-ray Diffraction

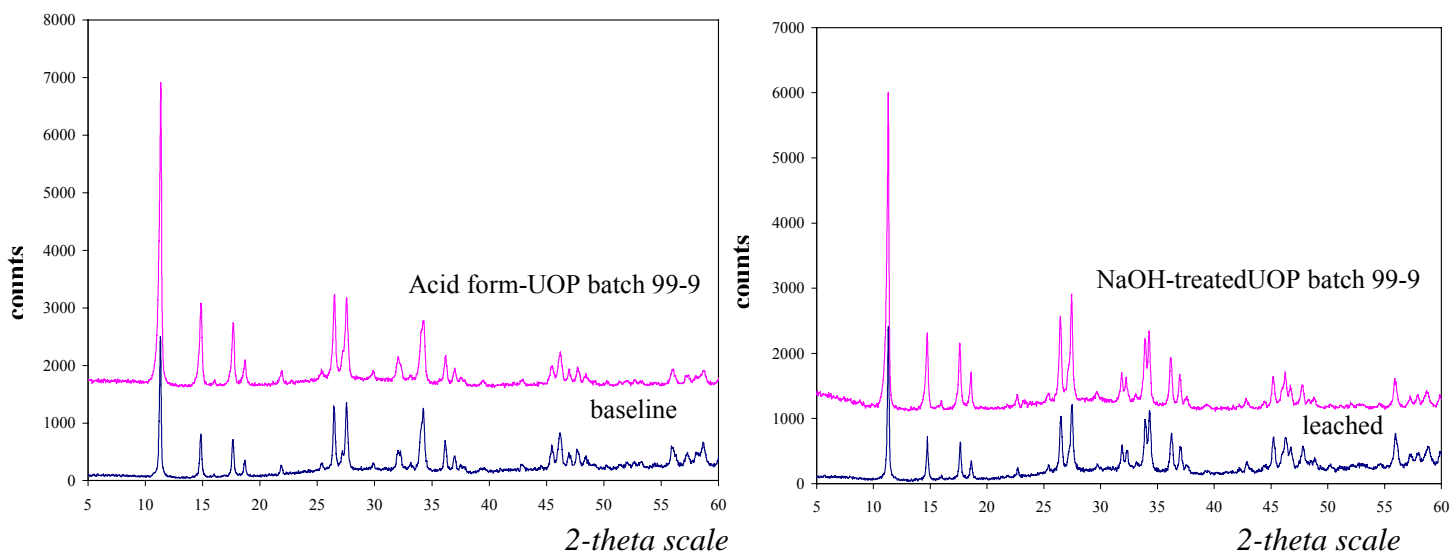


Figure 10. Powder X-ray diffraction spectra of baseline (left) and leached (right) IE-911, compared to the acid and base forms, respectively, of UOP batch 99-9.

Figure 10 shows the powder X-ray diffraction spectra of the baseline and leached forms of IE-911, compared to UOP batch 99-9, acid form and NaOH-treated form. There is essentially no difference between the 99-9 forms of IE-911 and the new baseline and leached forms. The apparent differences in intensity are due to the replacement of the X-ray detector between analyzing the 99-9 batches (10/00) and the new batches (2/01). All peaks observed in the baseline and leached materials belong to the CST phase, since the binder is amorphous. Further, no extra peaks are observed for the impurity phases observed by TEM (see below), which confirms the crystalline impurity phase (i.e. the niobium oxide) composes a very small fraction of the bulk material.

4.3 Infrared Spectroscopy (binder characterization)

The IR spectra of baseline, UOP-leached and UOP-leached and NaOH-treated IE-911 are shown in **figure 11**, focusing especially on characterization of the binder. There are some differences between these new IE-911 batches and the ‘old’ batch 98-7 (see figure 7). For the acid forms of IE-911, the surface carbonate band is extremely strong and sharp in the new baseline material compared to that of batch 98-7. This suggests that Zr(OH)₄ adsorption of carbonate is extremely sensitive to variations in manufacturing conditions which are unavoidable under normal operating procedures (i.e. purity of

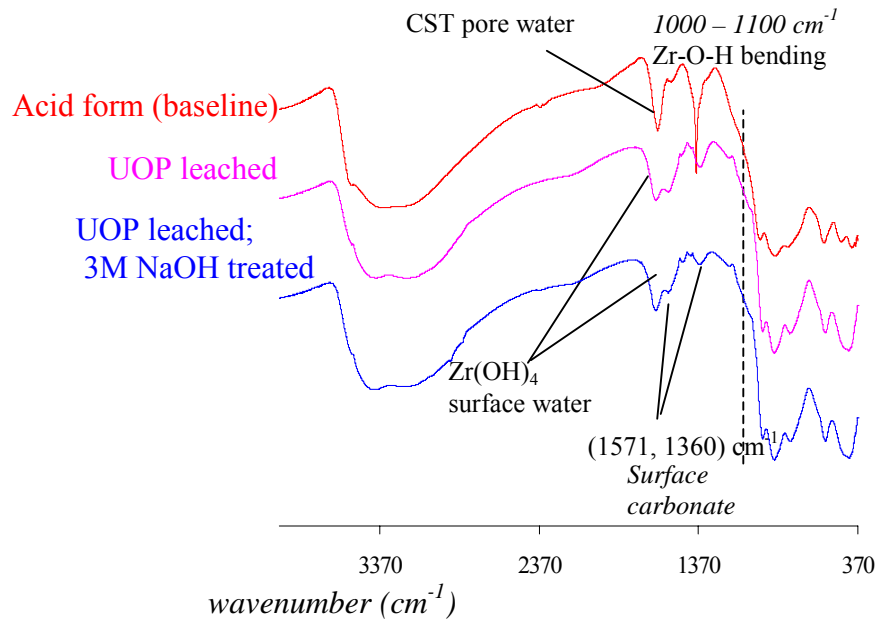


Figure 11. Infrared spectra of improved IE-911: baseline, UOP-leached and UOP-leached, NaOH-treated.

precursor materials, temperature, humidity, etc.). Otherwise, the same features are observed as previously described (section 4.3). That is, NaOH treatment of bound CST (IE-911) results in a decrease in surface carbonate anions, an increase in surface-bound water and a change in the Zr-OH bending region of the spectra.

4.4 Characterization of Morphology and Composition by Backscattering Electron Imaging (BEI) and X-ray Maps

Polished cross-sections of IE-911, baseline and leached, were prepared. Pellets and Gatan epoxy G-2 were combined in a 0.5 cm diameter plastic ‘bucket’. The sample was then vacuum-impregnated with the epoxy to ensure the porous pellets would remain intact during the subsequent polishing step. The epoxy is then cured at 100° C. A 1-millimeter slice of the epoxied sample was obtained by cutting with a diamond saw. Finally, the 0.5 x 1mm disc is polished on one side by 600 grit paper followed by a polish with a 1-micron diamond film. Epoxy-mounted samples were carbon-coated and mounted on a carbon disc prior to examination. Images and X-ray maps were obtained

on a JEOL JSM-T300 SEM utilizing the SEM in a backscattering-electron mode. Elements analyzed for included Na, Ti, Zr, Si and Nb. Maps were created from six composite parts of 256 scans each.

Figure 12 shows backscattering electron images of baseline and leached materials along with the maps for Ti, Zr and Nb. We focused on these three elements for X-ray maps because, together, they represent the composite, bound material. The Ti, which is heavier (thus more electrons) than Na or Si and therefore gives a better electron signal, was used to map out the location and relative concentration of CST throughout the pellets. Further, no Ti-containing impurities have been reported so a Ti X-ray map is a true representation of only CST. The Zr X-ray map directly reveals the relative concentration of binder throughout the pellets. The Nb X-ray maps reveal the variance of CST concentration throughout the pellets as well as Nb-containing impurities. It is clear from the images that the pellets are aggregates of higher- and lower- density agglomerations; the brighter regions are of higher density: the darker regions are of lower density. The X-ray maps reveal that the brighter agglomerates correspond with higher Zr concentration, or higher binder concentration. In the leached IE-911, the Ti (CST) concentration is qualitatively inverse to that of the Zr (binder). In other words, where the binder density is higher, the CST density is lower. This effect is not so evident in the baseline IE-911. This effect is likely to be an artifact of the analysis technique, rather than a real property of the material. The Nb density appears to mirror that of the binder and does not match the density of the Ti. This is likely because the L- α electron energies (which produce the X-ray maps) of Zr and Nb partially overlap, and therefore some Zr signal is picked up in the Nb X-ray map.

Higher magnification views of both baseline and leached IE-911 reveals the presence of sparse niobium-oxide impurities which are several microns in diameter and are dispersed randomly throughout the pellets. These niobium-oxide particles are estimated to compose less than 1% of the total pellet volume. Several examples of the niobium oxide impurities are shown below in **figures 13-15**, as backscattering electron images and Nb X-ray maps.

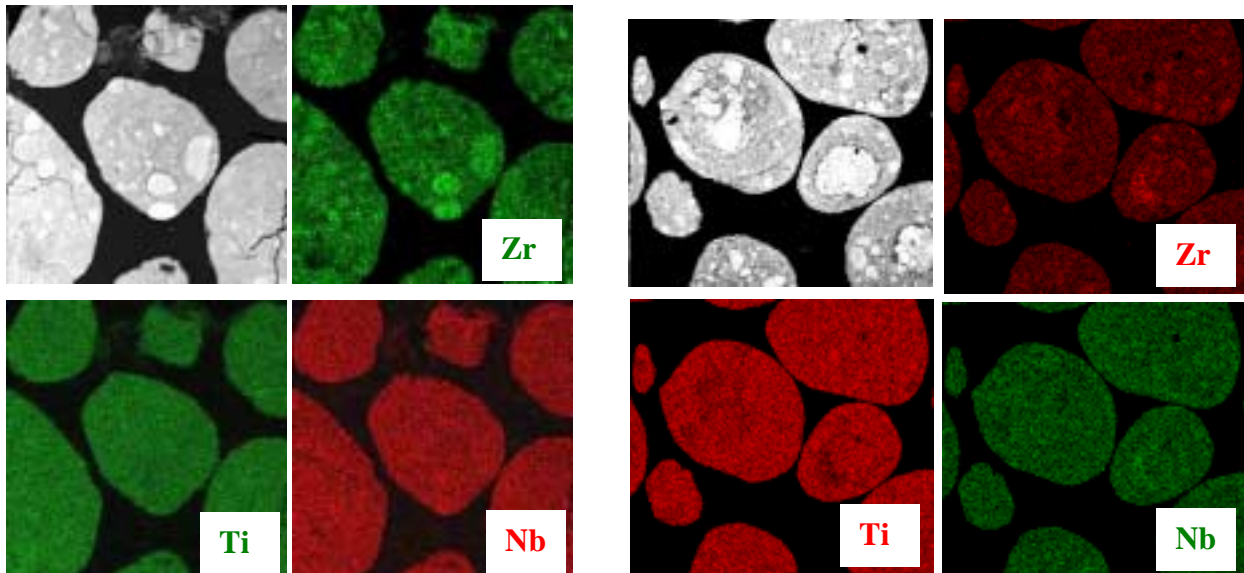


Figure 12. Backscattering electron images and Zr, Nb and Ti X-ray maps of baseline IE-911 (left) and leached IE-911 (right). Magnification = 200x for both.

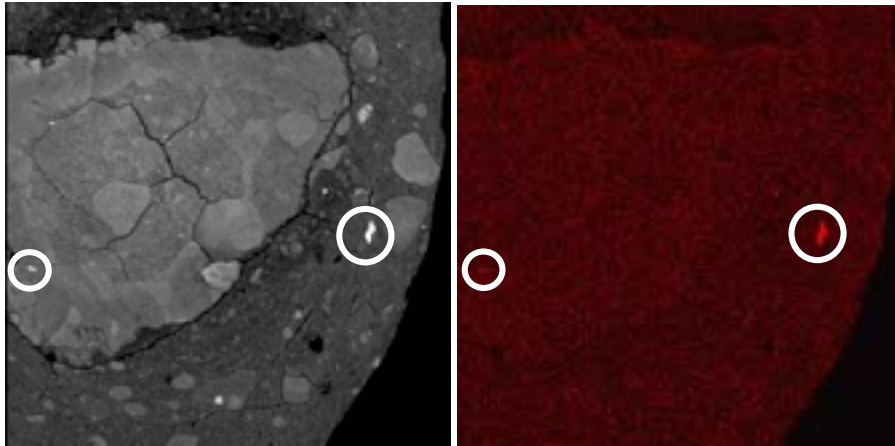


Figure 13. Backscattering-electron image (left) and Nb X-ray map (right) of leached IE-911 showing Nb oxide impurities, seen as bright areas in the image and red areas in the Nb X-ray map. Magnification = 500x.

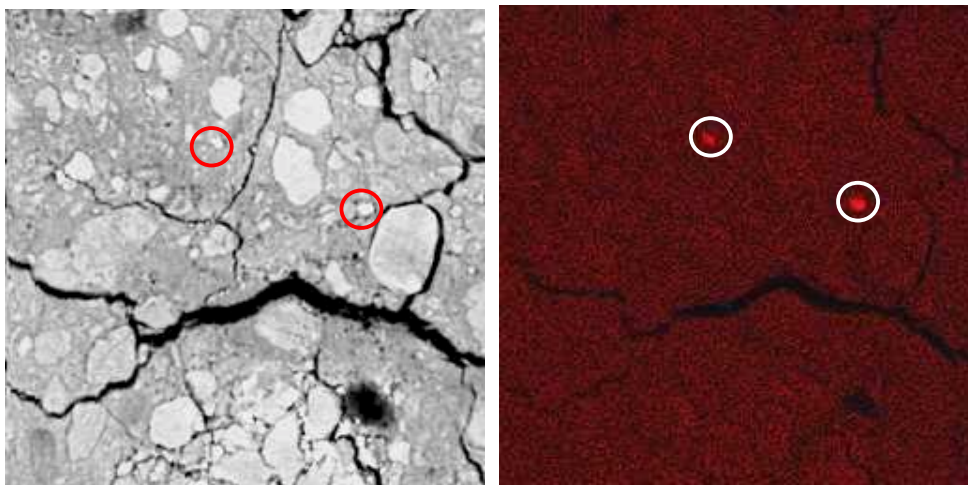


Figure 14. Backscattering-electron image (left) and Nb X-ray map (right) of baseline IE-911 showing Nb-oxide impurities. Magnification = 750x.

Conclusions for the BEI X-ray map studies can be summarized as follows:

- Pellets are a “conglomeration” of regions of high and low binder concentration
- In the baseline material, the CST density appears to be uniform throughout
- A small amount of Nb-O particles (several microns in size) is observed throughout both baseline and leached materials.

4.5 TEM studies of baseline and leached IE-911 silicon and niobium impurities.

As mentioned in the introduction, UOP has altered the IE-911 manufacturing process in order to address the problem of excessive Si and Nb leaching, which may result in in-column precipitation of aluminosilicate or niobate phases, respectively. The Nb and Si leach concentrations for UOP batch 99-9, baseline and leached IE-911 are summarized in **Table 2**.

Table 2. IE-911 Leachable Si and Nb.*

Material	Si (ppm)	Nb (ppm)
Batch 99-9 IE-911, acid	48.5	105
Baseline IE-911	31.5	72
Leached IE-911	28.3	5.25

*5 g. IE-911, 100 ml 3M NaOH, 48 hours. Data courtesy of Bill Wilmarth, SRTC

There is a significant decrease in leachable Nb from the old and new acid forms of IE-911 (from 105 to 72 ppm). Corresponding with this decrease, we observe about a 50% decrease in concentration of IPX in the baseline IE-911, compared to batch 99-9. The leached IE-911 shows essentially no Nb leaching, which is consistent with our observation that IPX is very sparse in this material. However, we do observe two additional Nb-containing phases. There is a niobium titanate phase (**figure 15a**) observed primarily in the baseline material and a crystalline niobium oxide (**figure 15b**) which is abundant in both the baseline and leached materials. The niobium titanate material appears to be similar to IPX in that it is a hydrated phase (releases water and decomposes under the electron beam) and is removed (dissolved) by a base treatment.

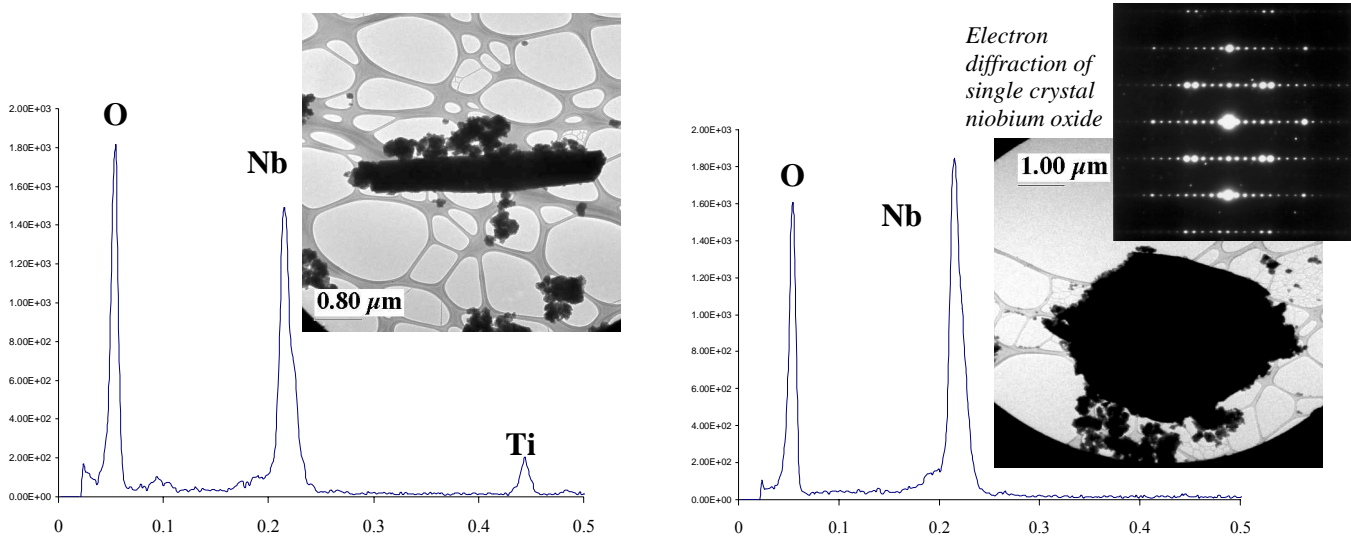


Figure 15. a. Ti-Nb-oxide impurity observed in baseline IE-911: TEM image and EDS spectrum (left). b. Crystalline Nb-oxide impurity abundant in both baseline and leached IE-911: TEM image, electron diffraction and EDS spectrum (right).

This phase is composed of very large crystals; it is observed optically in the baseline IE-911. On the other hand, the second ‘new’ niobium-based impurity, the niobium-oxide phase, is not extremely soluble in NaOH, in that it is still present in the leached IE-911. The niobium oxide phase is presumed to be the material observed in the BEI X-ray maps of the baseline and leached IE-911 cross-sectioned samples. The niobium oxide is identified as either Nb_2O_5 or $\text{Nb}_{12}\text{O}_{29}$ by electron diffraction, and is extremely crystalline, often single-crystal. In fact, its apparent low leachability may be related to its high crystallinity since amorphous niobium oxide exhibits much higher solubility than crystalline niobium oxide. Therefore, at least with regard to the question of column conditioning, this Nb-based impurity should not create a column-plugging problem.

However, how this impurity stands up to simulant or increased temperature or time of exposure remains presently unknown.

The decrease in leachable Si from old IE-911 (batch 99-9) to baseline IE-911 is significant (reduction of 40%) by leach tests (see Table 2), yet not readily observable by TEM. The Si impurities observed in the baseline and leached IE-911 are quite similar to those observed in batch 98-7, which were described previously. That is, amorphous silica is observed in the baseline material, often agglomerated with amorphous alumina. However, the crystalline aluminosilicate phase observed in the NaOH-treated batch 98-7 is not apparent in the leached IE-911. Perhaps the caustic wash implemented by UOP to produce the leached material is not basic enough to result in this reaction. Two examples of silica (**figure 16a**) and silica plus alumina (**figure 16b**) impurities in the baseline IE-911 are observed below.

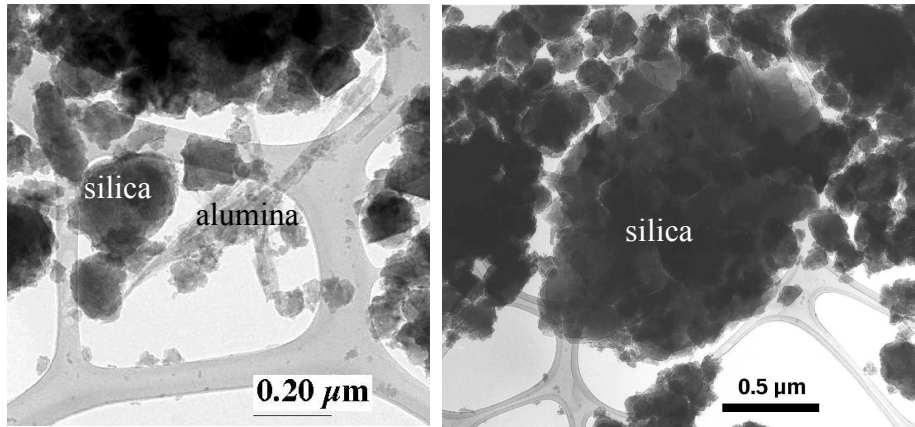


Figure 16. Two examples of alumina and silica impurities in pre-production, baseline IE-911: a. amorphous silica and fibrous alumina in baseline IE-911. (left) b. amorphous silica in baseline IE-911 (right)

In general, the form, composition, morphology, size and other characteristics of silica impurities are not really consistent from one batch to the next. It has been suggested that these impurities come from previous silicate and aluminosilicate syntheses at the UOP factory, which explains their inconsistencies.

5.0 Summary

This body of work has encompassed a variety of topics geared toward understanding performance issues of IE-911. A second focus of these studies is characterization of the pre-production IE-911 batches that had been revised to eliminate impurity phases that are likely to be the root cause of some of these performance issues. The first performance issue addressed in this study is the high concentrations of leachable Nb in UOP batches 98-5, 99-7 and 99-9. To address this issue, the major Nb-containing impurity phase (IPX) was identified and its ion-exchange and solubility properties were investigated. Based on these studies, it was determined that this source of leachable Nb must first be exposed to a pH=1 acid wash followed by a NaOH treatment in order to remove it. The acid wash was already implemented by UOP in the form of the binding process. Therefore, the addition of a caustic wash step by UOP in the batch mode resulted in successful removable of IPX. Finally, the addition of this caustic wash step produced a material with leachable Nb reduced by a factor of 20 over the previous acid-form material.

The binder material was also characterized and its behavior in NaOH solution was examined. These studies provided a documentation of the spectroscopic characterizations of the binder material that, in turn, gave a more complete picture of IE-911 as a whole. The composition of the binder was determined to be $Zr(OH)_4$. The binder material does exhibit some changes upon exposure to NaOH solution, as evidenced by changes in TGA-DTA and IR spectra. There is an increase in surface-bound, molecular water. There is also evidence for some cross-linking of the binder by 1) Base-catalyzed condensation reactions to form oxo- bonds; and/or 2) Local dissolution/precipitation of the zirconium hydroxide, producing a more ordered material by increasing the number of bridging hydroxyl groups. This type of cross-linking may either 1) increase the binder strength by formation of more bonds, or 2) decrease the binder strength by increasing brittleness upon exposure to NaOH solution.

Finally, a combination of backscattering-electron imaging and elemental X-ray mapping and TEM/EDS were used to document the Si and Nb impurity phases in the new baseline and leached IE-911. The Nb-based impurities observed in the baseline material included IPX, crystalline niobium oxide and a Ti-Nb-oxide phase. In the leached IE-911, the crystalline niobium oxide is prevalent but the IPX and Ti-Nb-oxide phases are removed. This crystalline niobium oxide appears to be abundant in the leached IE-911 but the leached IE-911 has minimal leachable Nb in NaOH solution. This suggests the crystalline niobium oxide is stable (i.e. not soluble) in NaOH solutions.

UOP's revised manufacturing processes did not have as drastic an effect on the composition, morphology or concentration of silica impurities. The leachable silica decreases by approximately 40% from the old to improved IE-911 batches. By TEM, we observed similar silica impurities in the old and new acid form-IE-911 batches, which may be sources of excess Si leaching. However, there are compositional and morphological inconsistencies in these impurities from batch to batch, and impurity to impurity. It has been suggested these impurities are picked up in the UOP factory from

previous silicate and aluminosilicate syntheses. It is our recommendation that these types of impurities which provide leachable silica sources should be minimized if possible. This suggestion is made in light of the fact that the simulant solutions (and therefore some waste solutions) are saturated with respect to Si, and with regard to aluminosilicate precipitation. Therefore, the presence of leachable silica sources such as these adds an uncertainty with regard to simulant and real waste solution stability in the presence of IE-911.

In conclusion, the major issues concerning performance of IE-911 (aluminosilicate precipitation and Nb-oxide column-plug precipitation) have been addressed by this effort and other efforts at Savannah River Site, Sandia National Laboratories, Pacific Northwest National Laboratory and Oak Ridge National Laboratory. With UOP's cooperation, the source of the Nb-oxide column-plug formation has been identified and eliminated. Although there is now a different Nb-containing impurity present in the improved IE-911, it appears to be stable to NaOH treatment. Current and future column and batch tests will evaluate its stability to more rigorous chemical treatment (i.e. simulant, increased time and temperature). Great inroads (particularly the efforts of Krumhansl et al, SNL and Su et al, PNNL), have also been made to understanding the source and cause of aluminosilicate precipitation. However, this issue still requires investigation for a full understanding of the cause and possible prevention of this performance issue.

6.0 Cited References

1. Anthony, R. G., Dosch, R. G., and Phillip, C. V., 6,110,378, Sandia National Laboratories, U.S.A. (August, 2000).
2. Walker, D. D., *Crystalline Silicotitanate Column Plugging Incidents*. Interoffice memorandum SRT-LWP-2000-00136, WSRC, Aiken, S.C. (1999).
3. Walker, D. D., Adamson, D. J., Allen, T. D., Blessing, R. W., Boyce, W. T., Croy, B. H., Dewberry, R. A., Diprete, D. P., Fink, S. D., Hang, T., Hart, J. C., Lee, M. C., Olsen, J. J., and Whitaker, M. J., *Cesium Removal From Savannah River Site Radioactive Waste Using Crystalline Silicotitanate (IONSIV® IE-911)*. WSRC-TR-99-308, WSRC, Aiken, S.C. (1999).
4. Welch, *Hydraulic Performance and Gas Behavior of Tall, Crystalline-Silicotitanate Ion-Exchange Column*. ORNL-TM-99-103, Oak Ridge National Laboratory, (1999).
5. Nyman, M., Headley, T., and Nenoff, T. M., *Characterizations of As-received, Pre-treated and Simulant-treated IE-911 (UOP batches 98-5, 99-7, 99-9)*. Interim Report, Sandia National Laboratories, Albuquerque, NM (2000).
6. Walker, D. D., *Pretreatment Guidelines*. SRTC-LWP-2000-0028:, Savannah River Site, Aiken, SC (1999).
7. Wester, D., *Tank Focus Area Savannah River Site Salt Processing Project Research and Development Program Plan*. PNNL-13253, PNNL, Richland, WA (2000).
8. Wilmarth, W. R., Dukes, V. H., Mills, J. T., and Fondeur, F. F., *Effect of Sodium Hydroxide Pretreatment of UOP IONSIV IE-911 Crystalline Silicotitanate Sorbent*. WSRC-TR-2000-00167, WSRC, Aiken, S.C. (2000).
9. Gu, D., TAM-5, A Hydrous Crystalline Silicotitanate for Removal of Cesium from Dilute Aqueous Waste, in *Kinetics, Catalysis and Reaction Engineering Laboratory, Department of Chemical Engineering, Texas A&M University, College Station, TX* (1995).
10. Greenlay, N., UOP Technical Exchange, SRTC, Aiken, S. C. (2000).
11. Krumhansl, J. L., Zhang, P.-C., Jove-Colon, C., and Anderson, H. L., *General Stability Models for Potential IE-911 Column Plugging Materials*. Sandia National Laboratories, Albuquerque, NM 87185 (2000).
12. Connor, P. A., Dobson, K. D., and McQuillan, A. J., "Infrared Spectroscopy of the TiO₂/Aqueous Solution Interface". *Langmuir* 15, p 2402 (1999).

13. Dobson, K. D., and Mcquillan, A. J., "An Infrared Spectroscopic Study of Carbonate Adsorption to Zirconium Dioxide Sol-gel Films from Aqueous Solutions". *Langmuir* 13, p 3392 (1997).
14. Nakamoto, K., *Infrared and Raman Spectra of Inorganic and Coordination Compounds*, p. Pages, John Wiley & Sons, New York (1986).
15. Brinker, C. J., and Scherer, G. W., *Sol-Gel Science*, p. Pages, Academic Press (1991).
16. Clearfield, A., "The mechanism of hydrolytic polymerization of zirconyl solutions". *J. Mater. Res.* 5, p 161 (1990).
17. Dosch, R. G., and Anthony, R. G., *Hydrous Crystalline Silico-Titanates: New Materials for Removal of Radiocesium from Concentrated Salt Solutions with pH's in the 1-14 Range , A Topical Report*. Sandia National Laboratories, Albuquerque, N.M. (1995).

7.0 Acknowledgements

Bill Wilmarth (SRTC) for Si and Nb leach data.

Paul Taylor (ORNL) for samples; particularly the UOP 98-5 and 99-7 batches.

Jim Krumhansl and PengChu Zhang (SNL) for assistance with the DCP spectrometer.

Michael Rye (SNL) for preparation of the IE-911 polished thin sections.

DISTRIBUTION LIST:

Sandia National Laboratories Personnel

Organization 6118, Mailstop 0750
Jim Krumhansl
Organization 6233, Mailstop 0755
May Nyman (5)
Organization 6233, Mailstop 0755
Tina Nenoff
Organization 6233, Mailstop 0755
D. S. Horschel
Organization 1822, Mailstop 1411
T. J. Headley
Organization 6803, Mailstop 0734
Larry Bustard
Organization 6118, Mailstop 0750
Hank Westrich
Organization 6118, Mailstop 0750
Carlos Jove-Colon
Organization 6118, Mailstop 0750
Department File

Technical Library: Organization 9616, Mailstop 0899 (2)
Central Technical Files: Organization 8945-1, Mailstop 9018
Review and Approval Desk: Organization 9612, Mailstop 0612
For DOE/OSTI

Non-Sandia National Laboratories Personnel

Yali Su
Battelle
Pacific Northwest National Lab
P.O. Box 999 / MS K8-93
Richland, WA 99352

Liyu Li
Battelle
Pacific Northwest National Lab
P.O. Box 999 / MS K8-93
Richland, WA 99352

Jim Buelt
Battelle
Pacific Northwest National Lab
P.O. Box 999 / MS K9-09

Richland, WA 99352

Dennis Wester

Battelle
Pacific Northwest National Lab
P.O. Box 999 / MS P7-25
Richland, WA 99352

Steve Schlahta, PNNL

C/o Westinghouse Savannah River Company
Building: 704-3N (Room: N302)
Aiken, SC 29808

Harry Harmon

C/o Westinghouse Savannah River Company
Building 704-3N (Room N111)
Aiken, SC 29808

Paul Taylor

Oak Ridge National Laboratory
1 Bethel Road (Building 4501)
Oak Ridge, TN 37831

Tim Kent

Oak Ridge National Laboratory
1 Bethel Road (Building 4501)
Oak Ridge, TN 37831

Bill Wilmarth

Savannah River Technology Corp.
Building: 773-42A (Room: 153)
Aiken, SC 29808

Doug Walker

Savannah River Technology Corp.
Building: 773-A (Room: B-124)
Aiken, SC 29808

Fernando Fondeur

Savannah River Technology Corp.
Building: 773-A (Room: B-124)
Aiken, SC 29808

Sam Fink

Savannah River Technology Corp.
Building: 773-A (Room: B-112)

Aiken, SC 29808

Roy Jacobs

Westinghouse Savannah River Corp.
Building: 704-3N (Room: S311)
Aiken, SC 29808

Jeff Pike

Westinghouse Savannah River Corp.
Building: 704-196N (Room: N401)
Aiken, SC 29808

Joe Carter

Westinghouse Savannah River Corp.
Building: 704-3N (Room: S151)
Aiken, SC 29808

Jim McCullough

U.S. Department of Energy, Savannah River
Building: 704-3N (Room: N380)
Aiken, SC 29808

Patricia Suggs

U.S. Department of Energy, Savannah River
Building: 704-3N (Room: 380A)
Aiken, SC 29808

John Reynolds

U.S. Department of Energy, Savannah River
Building: 704-3N (Room: N152)
Aiken, SC 29808

Rich Braun

UOP
25 East Algonquin Rd
Des Plaines, IL, 60017

Nan Greenlay

UOP
25 East Algonquin Rd
Des Plaines, IL, 60017

Dennis Fennelly

UOP Molecular Sieves, Suite 207
307 Fellowship Road
Mt. Laurel, N.J. 08054

